Multidimensional Calculation of Combustion in a Loop-Scavenged Two-Stroke Cycle Engine

B.Ahmadi-Befrui and H.Kratochwill

AVL List GmbH.
Kleiststrasse 48
A-8020 Graz
Austria

ABSTRACT

A multidimensional computational method is employed to investigate the combustion process and its dependence on the ignition location in a loop-scavenged, two-stroke cycle spark-ignition engine. The engine geometric compression ratio is 15:1 and the study pertains to the operating condition of 5000 rpm.

The pre-combustion flow and charge composition distributions were obtained through complete simulation of the gas-exchange and compression processes, taking into account the effect of 'back flow', due to pressure-wave oscillations in the scavenge system, on the in-cylinder flow and charge mixing.

The results show a strong remnant of the induction flow, with turbulence levels markedly higher than in four-stroke cycle engines, prevailing at the time of ignition. The flow persists throughout the combustion but the turbulence decays rapidly. There is strong interaction of the flow with the flame, during early combustion stages, causing its displacement and affecting the subsequent combustion development. It is found that the pre-combustion flow structure and the spark location are of major significance with regard to combustion characteristics.

INTRODUCTION

The characteristics of the flow and combustion processes in the loop-scavenged two-stroke cycle engines have become the subject of increasing interest and attention [1] owing to the recent revival of interest in this engine category for automotive application, and the realization of inadequate understanding of the important features of the in-cylinder flow and combustion processes and their inter-dependence on the dynamic characteristics of the scavenge system.

Traditionally, the steady flow test method has been utilized to probe geometrical aspects of the gas-exchange process and optimize the scavenge system design and layout for best scavenging efficiency. This practice, however, provides scant practical information about the flow and gas exchange characteristics under engine operating conditions. The reasons are the influence of large temperature and pressure differences between the scavenge and the cylinder charges and, in particular, the over-riding effect of pressure-wave oscillations in the scavenge-exhaust system on the in-cylinder flow and gas exchange characteristics [2]. Furthermore, the increasing evidence indicates that the combustion characteristics are likely more dependent on the in-cylinder flow structure, turbulence and mixing process, than on the scavenging efficiency [3,4].

Computational fluid dynamics offers an expedient means for investigation of the flow, gas exchange and combustion processes under realistic engine operating conditions, and identification of the important features and major underlying interactions. The recent efforts towards calculation of the flow processes in two-stroke cycle engines and assessment of the predictive accuracy of the method are evidence of the growing awareness of its potential in assisting engine research and development [2-6]. The experience - mostly drawn from the application of the method to four-stroke cycle engines - indicates that although the quantitative accuracy of calculations suffers from uncertainties in the flow boundary conditions and their intricate dependence on the engine geometric details and operating condition, nevertheless, the qualitative features, underlying processes and trends are well predicted [7-9].

The present paper describes application of a computational fluid dynamics method, the FMCS-code system [10,11], to the study of flow and combustion in a loop-scavenged two-stroke cycle spark-ignition engine. This work draws upon and complements a previous calculation of the flow, gas exchange and mixing processes, under realistic operating conditions, in this engine [2].

The aim of this work is to investigate the features of flame development and interaction with the pre-combustion flow field and to examine the influence of spark-plug location on combustion characteristics. The engine has a geometric compression ratio of 15:1 and the calculations pertain to the operating condition of 5000 rpm. The in-cylinder flow and charge distribution prior to combustion were obtained through multidimensional simulation of the complete gas-exchange and subsequent compression processes, in which resort was made to an unsteady gas dynamic and cycle

calculation method [12] to provide the initial and boundary conditions for the multidimensional calculations, under the operating condition of interest. This procedure enabled incorporation, into the multidimensional calculations, of all data pertinent to the operating engine, including the important pressure-wave oscillations in the scavenge system [2].

The paper first provides a brief description of the mathematical framework for modelling of inhomogeneous-charge combustion and the calculation method. Then the engine configuration and computational mesh, the boundary and initial conditions, and the ignition procedure are discussed. The predictions of the flow and flame propagation for two spark-plug locations - a central and an off-centre plug - are presented and the important features are underlined. Finally, the main findings of the study are summarized.

THE CALCULATION METHOD

A number of publications have described, in some detail, the FMCS-code system and its implementation practices [10,11]. Hence, only a brief description of the mathematical framework and the numerical solution method is provided.

The Mathematical Framework

The method solves the density-weighted ensemble-averaged (i.e. Favre-averaged) differential conservation equations of mass, momentum and stagnation enthalpy, in addition to the transport equations of the k-ε turbulence model, in three space dimensions and time. In the general case of inhomogeneous, partially-mixed combusting flows, additional differential transport/conservation equations for mixture fraction 'f', fuel mass-fraction 'Y_{Fu}', and an optional exhaust gas recycle mass-fraction 'Y_{EGR}' are solved, within the frame-work of simple chemically reacting system (SCRS) model [13], in order to determine the charge composition, thermodynamic state and the heat release rate. The conservative scalar variable 'f' is equivalent to the total (burned + unburned) fuel mass-fraction and thus a measure of the mixing between the air and the fuel ($0 \leq f \leq 1$) irrespective of the combustion process.

The combustion reaction is expressed, in accordance with the current practice, by the single-step irreversible global form

$$1 \text{ kg Fuel} + \frac{S}{0.232} \text{ kg } (0.232\ O_2 + 0.768\ N_2) \rightarrow (1+S) \text{ kg Products} + (3.31\ S) \text{ kg } N_2 \qquad (1)$$

where S is the stoichiometric oxygen requirement per unit mass of fuel (= 3.535 for the present case).

The Combustion Model

The determination of the mean rate of reaction R_{Fu} is a primary objective of combustion models for turbulent reacting flows [14]. In this study, a combustion model of the turbulence-mixing-controlled type, originally proposed by Magnussen & Hjertager [15], is adopted. Accordingly, the expression for the reaction rate is

$$R_{Fu} = \frac{C_{Fu}}{\tau} \rho \cdot \text{Min} \left(Y_{Fu}, \frac{Y_{Ox}}{S}, \frac{C_{Pr} \cdot Y_{Pr}}{1+S} \right) \qquad (2)$$

in which C_{Fu} and C_{Pr} are empirical coefficients; τ is the turbulence dissipation time-scale ($\tau = k/\varepsilon$); ρ is the mean mixture density; Min (...) is a 'minimum value of' operator, and Y_{Fu}, Y_{Ox} and Y_{Pr} denote mean concentrations of fuel, oxygen and products, respectively. The value of the empirical coefficient C_{Fu} is shown to depend on the turbulence and fuel parameters [14,16]. Hence C_{Fu} needs adjustment to reproduce the experimental data (normally the global fuel mass-fraction burned) for a given engine and fuel.

In the present calculations, the values of parameters C_{Fu} and C_{Pr} were optimized for the central spark-plug engine geometry. Subsequently, these were used for calculation of combustion in the eccentric spark-plug case. The values of the empirical coefficients C_{Fu} and C_{Pr} are given in Table 1.

The Solution Method

The differential equations are recast into the general curvilinear-orthogonal form and transformed to an Eulerian-Lagrangian coordinate system. This enables their solution on a body-fitted curvilinear orthogonal computational mesh with moving boundaries.

The differential equations are discretized, adopting the finite-volume method. The Euler-implicit temporal and hybrid central/upwind spatial differencing schemes are employed in order to ensure unconditional numerical stability. The solution of the implicit equations is advanced, from the initial conditions, in a time-marching method; at every time (or crank-angle) step, the algebraic system of equations is solved until convergence (residual error of 10^{-4}) is achieved.

THE APPLICATION DETAILS

Engine Geometry and Computational Mesh

The engine is a 250 cc single-cylinder, crank case-scavenged high speed production unit. It has been used for research and development of alternative charge preparation and combustion concepts at AVL-List GmbH and is comprehensively reported in [12]. The engine geometric data and operating conditions are given in Table 1.

The computational mesh of the cylinder is illustrated in figure 1(a). The arrangement of the intake ports around the cylinder liner is symmetric with respect to the diametrical plane through the exhaust port; thus, the calculation domain is confined to half the cylinder volume. The details of the intake and exhaust port geometry and arrangment, pertinent to the simulation of the gas-exchange process, can be found elsewhere [2].

The computational mesh in figure 1(b) is used for the present combustion calculations and contains 7x20x34 (axial, radial, circumferential) cells in the cylinder and 8x14x34 cells in the cylinder head cavity. The locations of spark plugs (for the two study cases) and the planes selected for presentation of the results are indicated in figure 1(b). These are K-planes: K = 5 and 33, and I-planes: I = 2,4,7,11 and 13.

GEOMETRIC AND OPERATING DATA		
Bore	67.5	mm
Stroke	69.0	mm
Exhaust port opening	85	°ATDC
Scavenge port opening	121	°ATDC
Compression ratio	15:1	
Speed	5000	rpm
Mean piston speed $\bar{V}_p$	11.5	m/s
COMBUSTION DATA		
Ignition time	20	°BTDC
Ignition delay (1 % mfb)	11	°CA
Model coefficient C_{Fu}		
Combustion delay (0- 5 %)	C_{Fu} = 12	
Main combustion (5-99 %)	C_{Fu} = 20	
Model coefficient	C_{Pr} = 0.5	

Table 1: The engine and combustion data

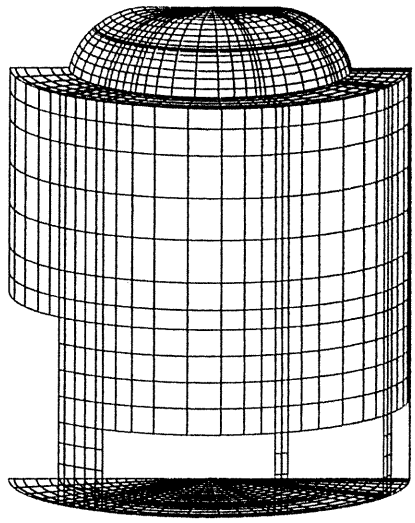

Fig. 1(a) Engine configuration and computational mesh

The I-planes are presented in perspective view, but the velocity vectors are the normal projections of the three-dimensional velocity field onto these planes; thus the vector lengths are independent of the perspective representation of the geometry.

Initial and Boundary Conditions

The initial conditions, i.e. the velocity field and distributions of the thermodynamic, composition and turbulence quantities at the time of ignition CA = 340 deg., were obtained through complete simulation of the gas-exchange and compression processes, in which a prior unsteady gas dynamic calculation [12] provided the initial and boundary conditions for the multidimensional calculations, under the operating condition of interest [2]. The most noteworthy feature of the pre-combustion flow simulation, with respect to the present study, was the evidence of the over-riding effect of the 'back flow', caused by pressure oscillations in the scavenge system, on break-up of the in-cylinder scavenge-loop flow structure and consequent enhanced charge mixing [2].

The boundary conditions are the no-slip velocity and constant temperature condition at the walls. The cylinder head, liner and piston temperatures are assigned values of 570 K, 470 K and 500 K, respectively. The standard law-of-the-wall is adopted in the turbulence equations to bridge the low-Reynolds number near-wall region.

Ignition Procedure

The ignition is simulated through burning of the fuel in a small volume around the spark location, at a prescribed rate proportional to the ignition delay period (i.e. duration of 1 % mfb).

The ignition locations, for the two study cases, are marked in figure 1(b). The ignition volume for both cases is 33 ± 0.2 mm³, containing 0.25 % of the total fuel in the charge. The fuel content of the ignition volume is depleted in a progressive manner over an ignition duration of 2.7° crank angles, equivalent to the experimental ignition delay (1 % mfb) of 11° crank angles.

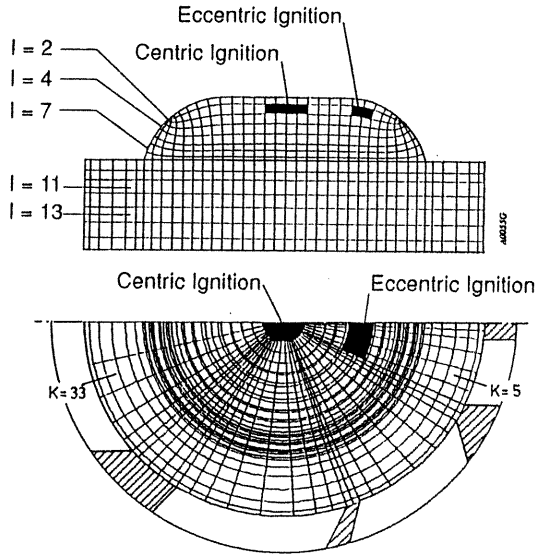

Fig. 1(b) The computational mesh, ignition volumes and planes of illustration of the results

Calculation Procedure

The calculations commenced at CA = 340 deg., the time of ignition, and were continued till complete combustion of the in-cylinder charge (i.e. 99 % mfb). A computational time-step, equivalent to $\Delta\theta$ = 1/32 degree crank angle was used throughout the calculations.

RESULTS AND DISCUSSION

This section is seperated into three parts. First, the variations of some important global (volume-mean) thermodynamic, combustion and flow parameters for the two study cases are discussed. Then, the multidimensional predictions of the flow and flame development for the cases of central and off-centre ignition location are presented and the important features are analysed.

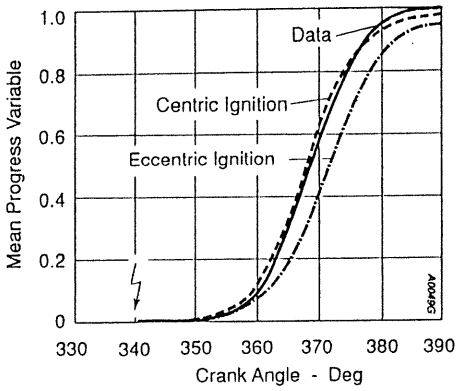

Fig. 2 The cylinder volume-averaged mean progress variable $\bar{C}$

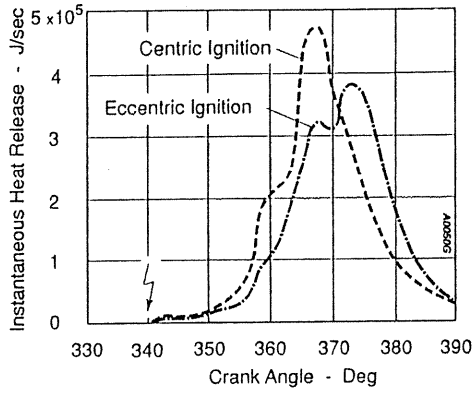

Fig. 3 The variations of the instantaneous heat release rate $\dot{Q}$

Global Parameters

The data (measurement and results from an unsteady gas dynamic and cycle program [12]) and the predicted variations of some important global combustion parameters, namely the volume-averaged mean progress variable $\bar{C}$ (i.e. the fuel mass-fraction burned normalized by the total fuel mass-fraction), instantaneous heat release rate $\dot{Q}$, cylinder pressure and normalized turbulence intensity, for the two study cases, are presented in figures 2 to 5, respectively.

The variations of $\bar{C}$ and $\dot{Q}$ show distinct differences between the global combustion characteristics of the central and off-centre ignition location. These indicate a markedly slower reaction, especially before CA = 370 deg., for the case of off-centre ignition; but the analysis of the multidimensional flame propagation reveals that the difference between the two cases is unrelated to the flame geometrical parameters and is caused by distinct flow-flame interactions. The predicted variation and time of peak cylinder pressure in figure 4 shows the extent of agreement with the data; the notable difference in the magnitudes may be attributed to differences in the thermodynamic properties and heat transfer rates between the cycle program [12] and the present method.

The most noteworthy results are the variations of the volume-averaged normalised turbulence intensity $u'/\bar{V}_p$ (where $\bar{V}_p$ is the mean piston speed) in figure 5. These show a notably high mean turbulence level of $u' \simeq \bar{V}_p$ at the time of ignition, that rapidly decays throughout the combustion period. There is indication of influence of combustion on the turbulence level (through affecting the flow and turbulence generation rate) but no evidence of marked turbulence augmentation.

Case I: Central Ignition Location

The velocity, turbulence intensity and mixture fraction distributions at the time of ignition, CA = 340 deg., are presented in figures 6(a) to 6(c), respectively. These show a strong ($U \simeq 3.\ \bar{V}_p$) complex vortical flow structure, which is the remnant of the scavenge loop-flow, its transformation into a tumbling motion through

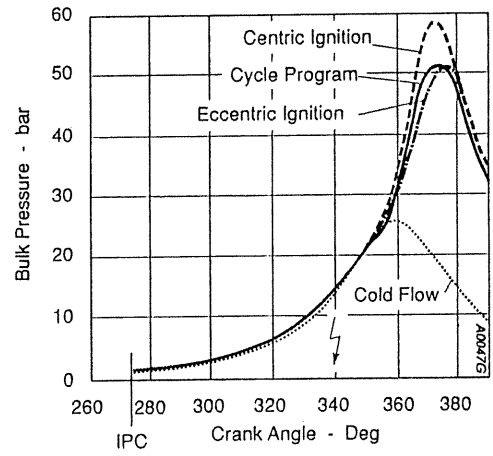

Fig. 4 The variations of the cylinder pressure

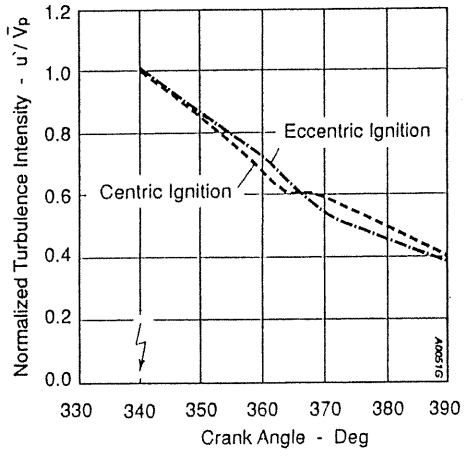

Fig. 5 The variations of the cylinder volume-averaged normalised turbulence intensity $u'/\bar{V}_p$

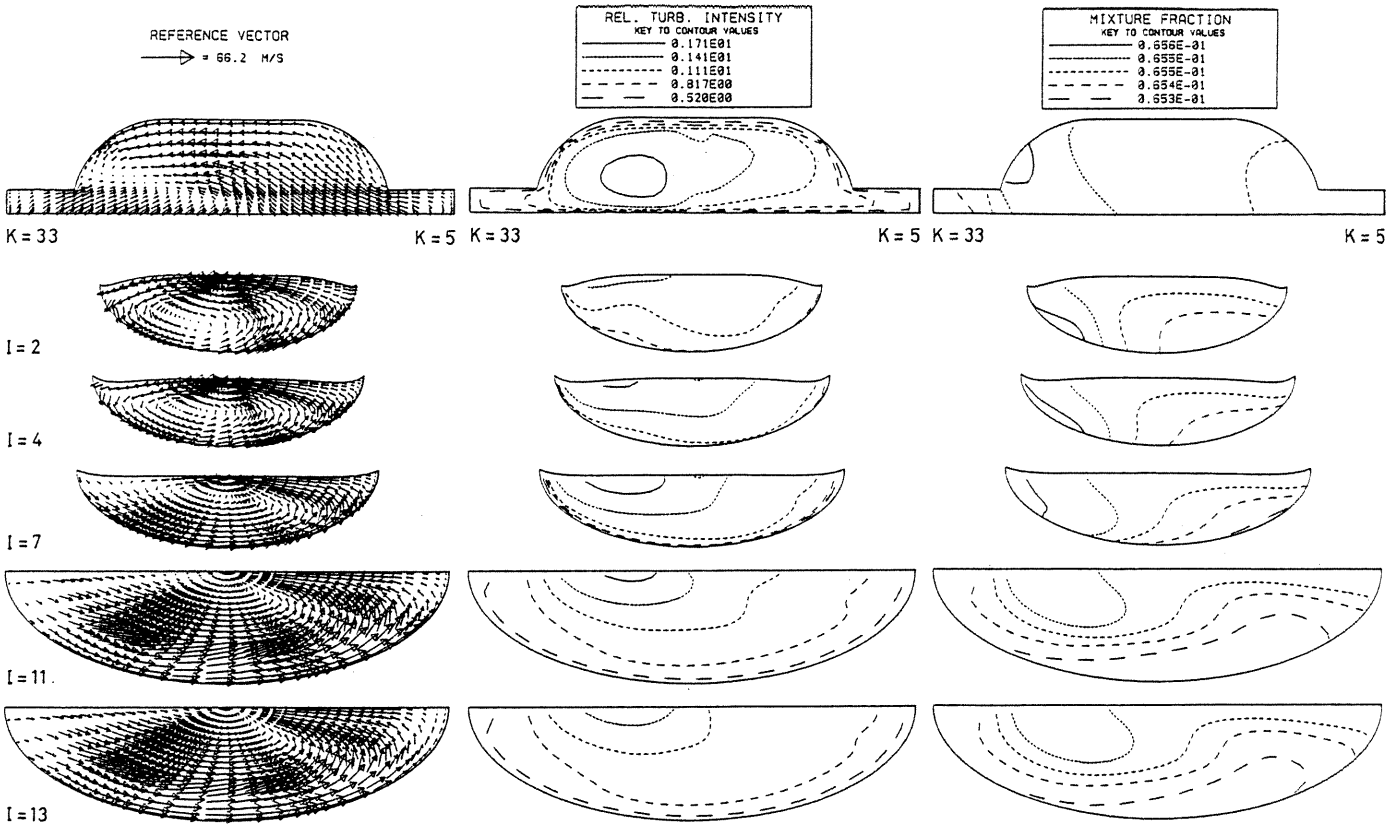

Fig. 6 The initial conditions at CA = 340°
(a) velocity field
(b) turbulence intensity $u'/\bar{V}_p$
(c) mixture fraction f

interaction with the pressure-wave induced 'back-flow' from the exhaust port, and further break-up through compression and effect of the squish-flow [2]. The turbulence intensity distribution, in figure 6(b), shows peak levels of $u'/\bar{V}_p$ = 1.5 - 1.7 within the cylinder-head cavity, markedly larger than turbulence levels, around the time of ignition, in four-stroke cycle engines [17]. This appears to be in part a consequence of the short time for the decay of intake turbulence in the two-stroke cycle engines, and additionally the significant turbulence generation due to spin-up of the tumbling flow structure. The in-cylinder charge is uniform, as evidenced in figure 6(c), owing to the break up of the scavenge loop-flow and high level of turbulent mixing.

The development of the flow and combustion is depicted in figures 7 to 9, presenting the plots of the velocity field and the reaction fluctuation intensity $\overline{C''^2}$ distribution at crank angles CA = 355, 365 and 380 degrees, respectively. It is worth pointing out that $\overline{C''^2} = \bar{C}(1-\bar{C})$ (in premixed combustion with fast chemistry [18]), where $\bar{C}$ is the reaction progress variable, is a normalized reaction rate in the range $0 \leq \overline{C''^2} \leq 0.25$, and hence is representative of the flame location.

The velocity field at CA = 355 deg. in figure 7(a) shows the influence of the non-uniform squish flow caused by the remnant of the loop-flow structure and formation of vortices 'A' and 'B'. There is notable influence of combustion on the detailed flow structure, but the heat release is insufficient to break up the strong vortex motion 'D'. However, the distribution of $\overline{C''^2}$ in figure 7(b), reveals major influence of the flow on the flame development: the flame has been convected from its initial cylinder-centre location by the strong flow remnants of the scavenge loop-flow and resides near the periphery of the cylinder-head cavity, on the side of the exhaust port. It is noteworthy that, as evidenced by figures 7(a) and 7(b), the squish flow 'C' plays an important role in stabilizing the flame, through inhibiting its propagation, counteracting its further displacement by the loop-flow remnant, and thus containing the flame in the cylinder-head cavity.

The results at CA = 365 deg., in figures 8(a) and 8(b), reveal the paramount effect of the initial flame displacement on its subsequent development. The velocity field in figure 8(a) shows that although the loop-flow structure is disintegrated, still components of its vortical motion in the radial-circumferential plane persist. The nature and extent of interaction of the vortical motion 'D' with the flame development are illustrated in figure 8(b), that shows the flame propagation into the clearance gap, at the location of initial flame displacement, and rapid circumferential development with the aid of flow 'D'. The rapid flame propagation, evidenced also by the large rate of increase of the global combustion parameters in figures 2 to 4, causes the break-up of the flow structure. However, the adverse effect of the persistance of the diametrical flow 'E' is evidenced by hindrance of the flame development near the centre of the cylinder.

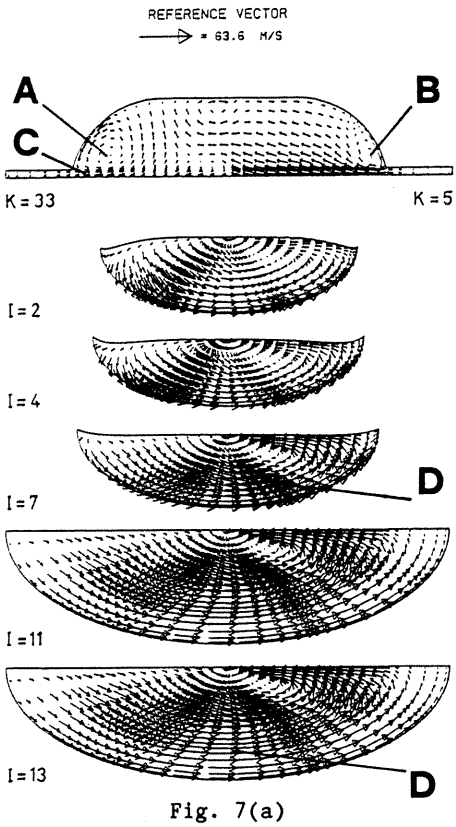

Fig. 7(a)

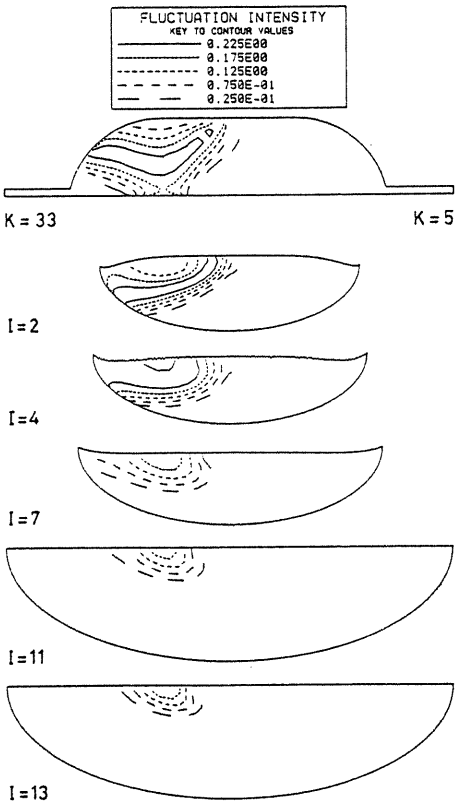

Fig. 7(b)

Fig. 7 The results for Case I at CA = 355°
(a) velocity field
(b) reaction fluctuation intensity $\overline{C''^2}$

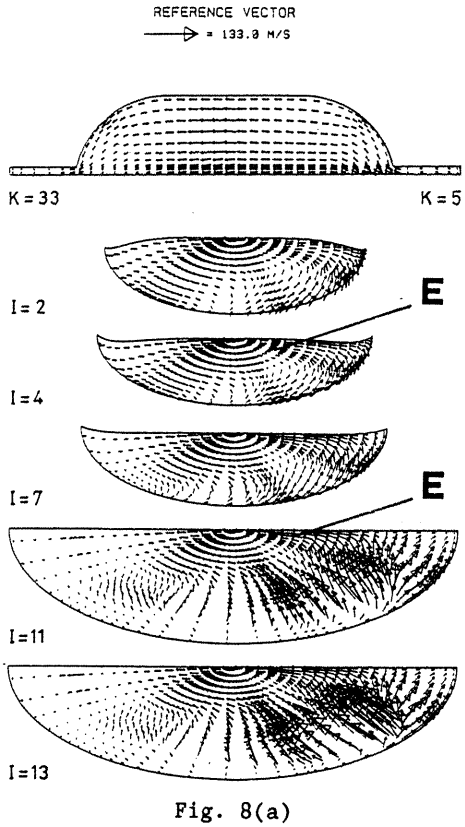

Fig. 8(a)

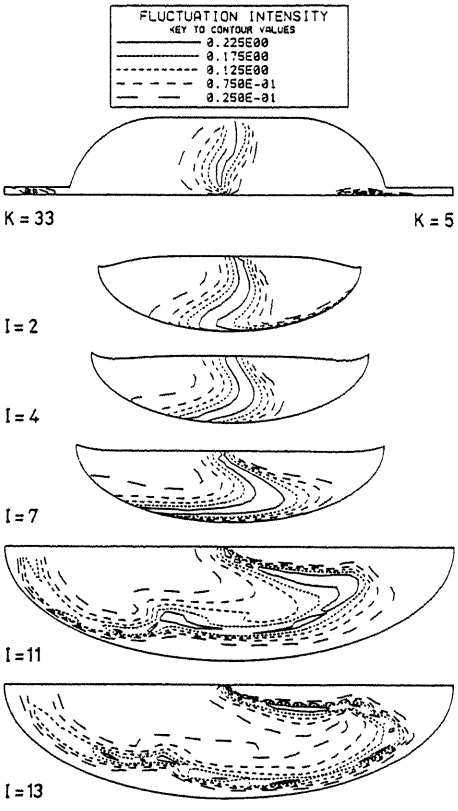

Fig. 8(b)

Fig. 8 The results for Case I at CA = 365°
(a) velocity field
(b) reaction fluctuation intensity $\overline{C''^2}$

The results at CA = 380 deg. pertain to the late combustion stage (mfb ≃ 92 %). The velocity field in figure 9(a) shows re-formation of a noticeably strong vortical motion ($U \simeq 3.\bar{V}_p$), through expansion of the non-uniform flame-induced flow. The distribution of the reaction intensity $\overline{C''^2}$ shows the completion of flame development in the cylinder and the on-going combustion at the surface of a pocket of unburned charge trapped in the cylinder-head cavity, above the location of the scavenge ports. This complex flame development is a consequence of multiple flame interactions with the flow, especially its rapid peripheral propagation through assistance of the vortex motion 'D' and reverse-squish, and retardation near the cylinder-centre by flow 'E'.

The initial flame displacement by remnants of the scavenge loop-flow and the subsequent flow interactions with the flame are of particular importance for the two-stroke cycle engines, because:

(i) the time for the decay of intake flow is short and hence the flow around the time of ignition is notably strong, and

(ii) the dependence of the in-cylinder flow structure on the strength and timing of the 'back flow', caused by pressure oscillations in the scavenge system [2], renders the combustion characteristics influenced by the engine operating condition.

It is significant that squish flow assists combustion stabilization, through opposing extreme flame displacement and containing it in the cylinder-head cavity. It is also noteworthy that a strong vortical flow structure is present at the end of combustion that will interact with the ensuing gas exchange process.

Case II: Off-Centre Ignition Location

The particular pattern of flame development in Case I lead to investigation of the off-centre spark plug location, in order to offset the effect of initial flame displacement by the flow.

The predictions of the flow and flame development are presented in figures 10 to 12, depicting the velocity field and distributions of the reaction intensity $\overline{C''^2}$, at the selected crank angles CA = 355, 365 and 380 degrees, respectively. The focus of the analysis of the results is on underlining the important features of the combustion and the differences with Case I.

The results at CA = 355 deg., in figures 10(a) and 10(b), show the displacement of the flame, from the ignition location towards the cylinder-centre, by the remnant of the loop-flow. There is insignificant influence of the combustion on the flow. The major features of the flame-development, namely the marked flame displacement by the flow and the weak effect of combustion on the strong flow structure are similar to Case I; although the details are different, owing to the flame location.

The results at CA = 365 deg., in figures 11(a) and 11(b), show a markedly different flow and flame development pattern from that of Case I. A semi-spherical flame occupying a significant portion of the cylinder-head cavity is established near the cylinder centre and is interacting with and majorly modifying the pre-ignition flow field.

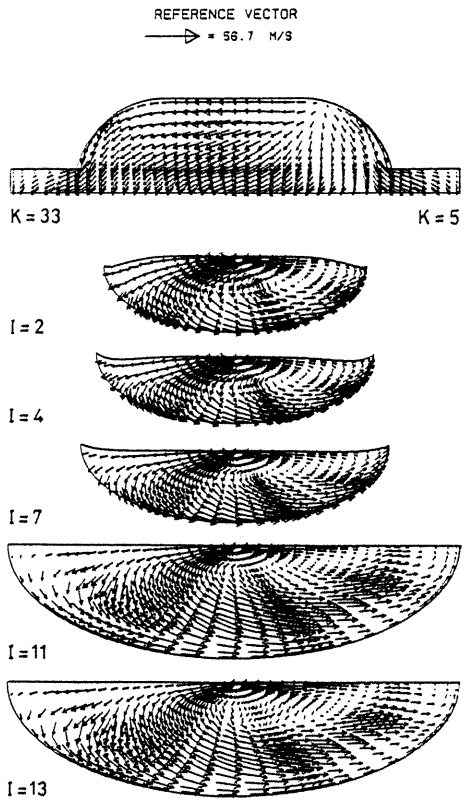

Fig. 9(a)

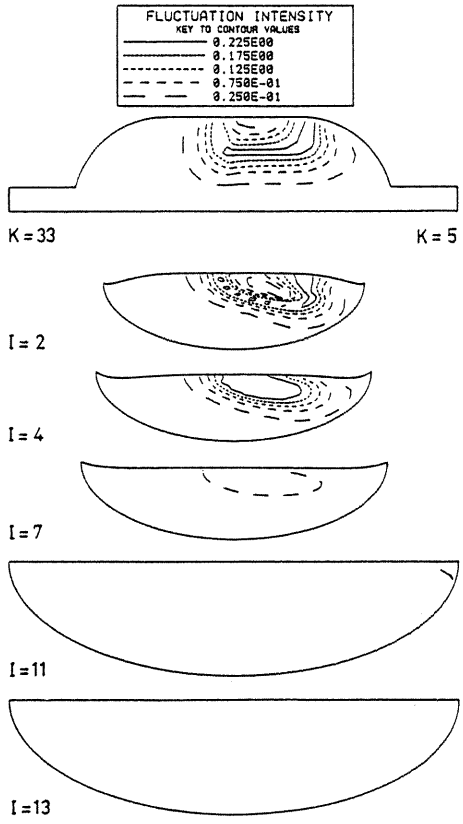

Fig. 9(b)

Fig. 9 The results for Case I at CA = 380°
(a) velocity field
(b) reaction fluctuation intensity $\overline{C''^2}$

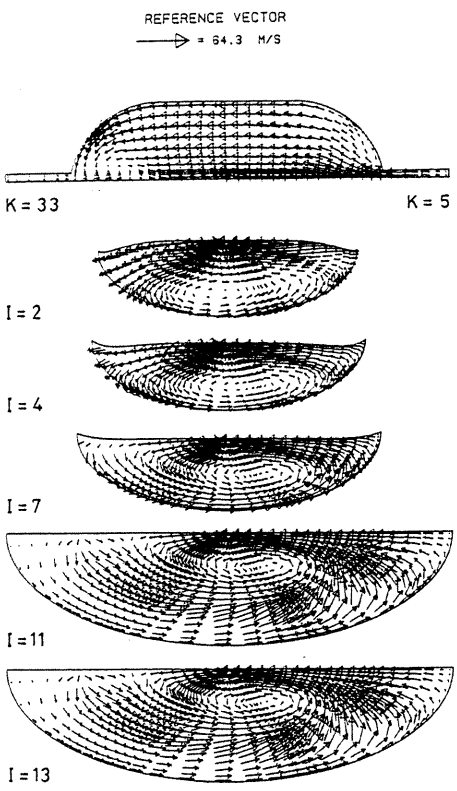

Fig. 10(a)

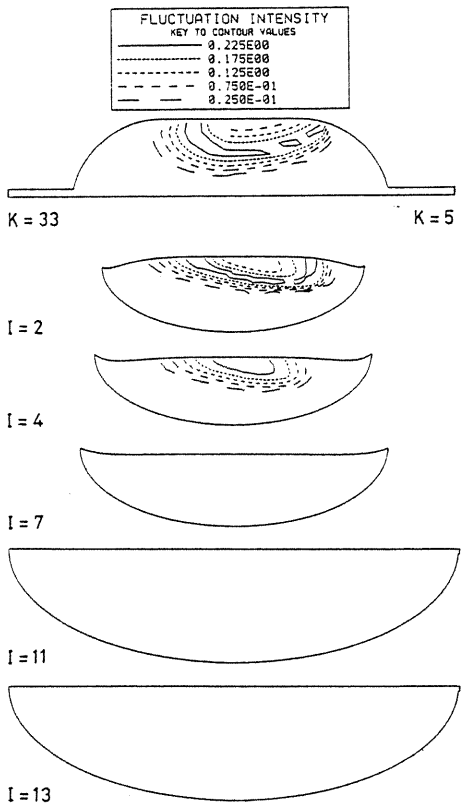

Fig. 10(b)

Fig. 10 The results for Case II at CA = 355°
(a) velocity field
(b) reaction fluctuation intensity $\overline{C''^2}$

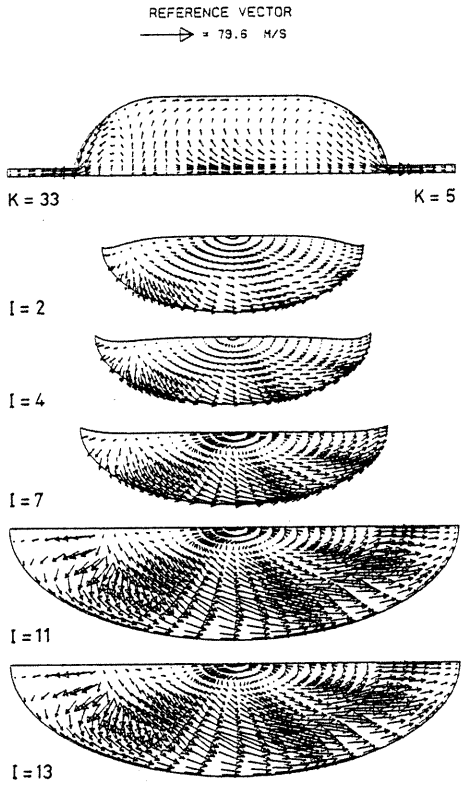

Fig. 11(a)

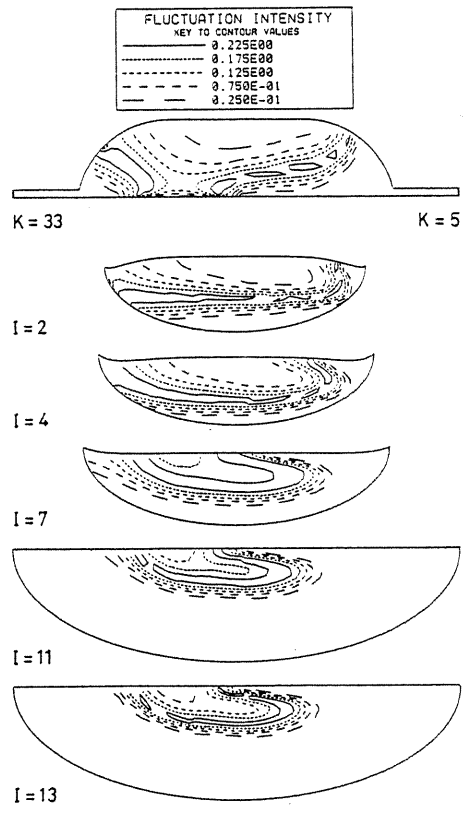

Fig. 11(b)

Fig. 11 The results for Case II at CA = 365°
(a) velocity field
(b) reaction fluctuation intensity $\overline{C''^2}$

This indicates that beyond a certain flame size, the heat release is sufficient to locally counteract the pre-combustion flow and render a stationary flame.

The results at CA = 380 deg., in figures 12(a) and 12(b), show the progress and completion of the flame propagation in the cylinder-head cavity, in advance of its development in the cylinder and clearance gap region, in contrast to Case I. However, similar to Case I, there is evidence of reformation of the strong vortical motion, due to the eccentric location of the reaction region in the cylinder.

These results indicate complex dependence of the flame development on the pre-ignition flow and spark-plug location. It is noteworthy that certain features of the flame pattern and flow structure - notably the strong flow and consequent flame retardation near the cylinder centre - demonstrate dependence on the imposed diametrical symmetry, that may be expected to become invalid due to flame asymmetries during combustion in practice. Although it has not been possible to assess the calculations through comparison with measurements, their overall trends, especially with regard to the influence of spark-plug location, is in agreement with experimental findings [19].

SUMMARY AND CONCLUSIONS

The main findings of the present investigation of the combustion in a loop-scavenged, two-stroke cycle spark-ignition engine are:

(i) A strong remnant of the induction loop-flow, with high turbulence level of order $u' \simeq 1.5 \overline{V}_p$, is present at the time of ignition. The flow may persist throughout the combustion, but turbulence decays at rapid rates.

(ii) The strong interaction of the remnant of the loop-flow with the flame, especially at early combustion stages, markedly affect the flame development pattern.

(iii) The location of the spark-plug is of major importance with regard to flow-flame interaction and hence the combustion characteristics.

(iv) Owing to the dependence of the in-cylinder flow structure on the strength and timing of the 'back-flow', the variations of engine operating condition may accompany notable changes of combustion characteristics.

The present study indicates that despite the limitations of the current model of turbulent combustion for spark-ignition engines, computational fluid dynamics offers a unique means for investigation of the characteristics of the flow and combustion processes in the loop-scavenged two-stroke cycle engines. Already, research studies are underway to investigate the influence of flow efflux-angle on the scavenging characteristics and examine the semi-direct (port) and direct (in-cylinder) fuel injection methods [12,20] with regard to charge preparation, homogeneity at the time of ignition and combustion.

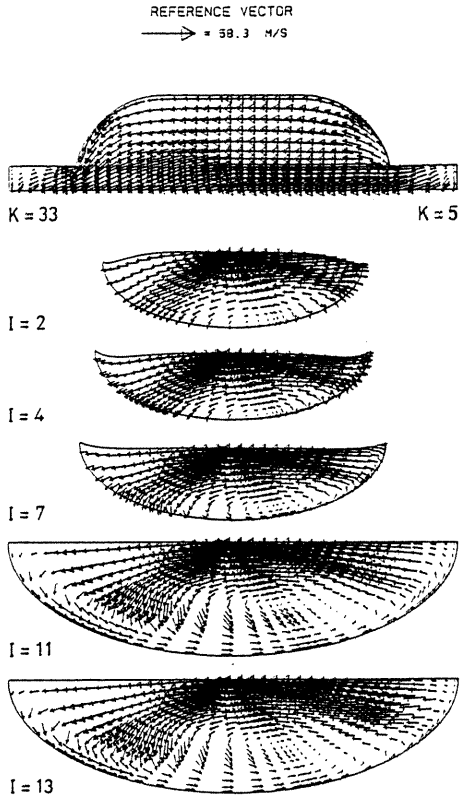

Fig. 12(a)

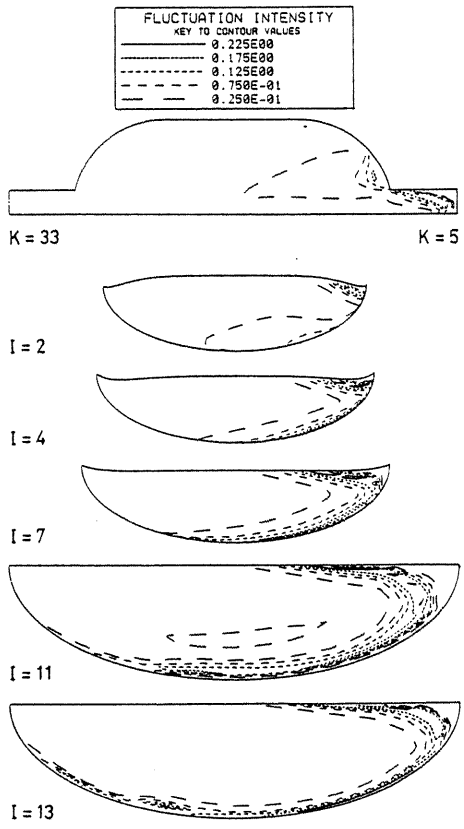

Fig. 12(b)

Fig. 12 The results for Case II at CA = 380°
(a) velocity field
(b) reaction fluctuation intensity $\overline{C''^2}$

REFERENCES

1. Blair, G.P. (ed.), "Advances in Two Stroke Engine Technology", SAE PT-33, 1988.

2. Ahmadi-Befrui, B., Brandstätter, W. and Kratochwill, H., "Multidimensional calculation of the flow processes in a loop-scavenged two-stroke cycle engine", SAE paper 890841, 1989.

3. Sweeney, M.E.G., Swann, G.B.G., Kenny, R.G. and Blair, G.P., "Computational fluid dynamics applied to two-stroke engine scavenging", SAE paper 851519, 1985.

4. Sher, E., "Modeling the scavenging process in the two-stroke engine - an overview", SAE paper 890414, 1989.

5. Schwarz, M.P., Thornton, G.J. and Gilbert, W., "In-cylinder flow simulation for a motored two-stroke engine", in G. De Vahl Davis and C. Fletcher (Eds.), Computational Fluid Dynamics, Proc. International Symposium on Computational Fluid Dynamics, Sydney, Australia, 1987, Elsevier Science Publishers B.V., 1988.

6. Smyth, J.G., Kenny, R.G. and Blair, G.P., "Steady flow analysis of the scavenging process in a loop-scavenged two-stroke cycle engine - a theoretical and experimental study", SAE paper 881267, 1988.

7. Ahmadi-Befrui, B., "Analysis of flow evolution in the cylinders of motored reciprocating engines", PhD Thesis, University of London, 1985.

8. Gosman, A.D., Tsui, Y.Y. and Vafidis, C., "Flow in a model engine with a shrouded valve - a combined experimental and computational study", SAE paper 850498, 1985.

9. Henriot, S., LeCoz, J.F. and Pinchon, P., "Three dimensional modelling of flow and turbulence in a four-valve spark ignition engine - comparison with LDV measurements", SAE paper 890843, 1989.

10. Johns, R.J.R., "A unified method for calculating engine flows", ASME-84-GDP-1P, 1984.

11. Brandstätter, W. and Johns, R.J.R., "Computer simulation of external and internal turbulent flows in the automotive industry", in C. Marino (Ed.), Supercomputer Applications in Automotive Research and Development, Proceedings of the Int. Conf. in Zurich, October 1986, Cray Research Inc.

12. Plohberger, D., Mikulic, L.A. and Landfahrer, K., "Development of a fuel injected two-stroke gasoline engine", SAE paper 880170, 1988.

13. Spalding, D.B., "Combustion and Mass Transfer", Pergamon Press, 1979.

14. Borghi, R., "Turbulent combustion modelling", Prog. Energy Combust. Sci., Vol. 14, 245-292, 1988.

15. Magnussen, B.F. and Hjertager, B.H., "On mathematical modelling of turbulent combustion with special emphasis on soot formation and combustion", 16th Symp. (Int.) on Combustion, The Combustion Institute, 719-729, 1977.

16. Cant, R.S. and Bray, K.N.C., "Strained laminar flamelet calculations of premixed turbulent combustion in a closed vessel", 22nd Symp. (Int.) on Combustion, The Combustion Institute, 1988.

17. Arcoumanis, C. and Whitelaw, J.H., "Fluid mechanics of internal combustion engines - a review", Pro. I.Mech.E., Vol. 201, No. C1, 57-74, 1987.

18. Bray, K.N.C., "Turbulent Flows with Premixed reactants", in P.A. Libby & F.A. Williams (Eds.), Turbulent Reacting Flows, Springer Verlag, 1980.

19. Plohberger, D., Private Communication, 1990.

20. Landfahrer, K., Plohberger, D., Alten, H., Mikulic, L.A., "Thermodynamic analysis and optimization of two-stroke gasoline engines", SAE paper 890415, 1989.